Longitudinal analysis of heart and liver iron in thalassemia major

Leila J. Noetzli,[1] Susan M. Carson,[2] Anne S. Nord,[2] Thomas D. Coates,[2] and John C. Wood[1,3]

[1]Department of Pediatrics, Division of Cardiology, [2]Division of Hematology-Oncology, and [3]Department of Radiology, Childrens Hospital Los Angeles, CA

High hepatic iron concentration (HIC) is associated with cardiac iron overload. However, simultaneous measurements of heart and liver iron often demonstrate no significant linear association. We postulated that slower rates of cardiac iron accumulation and clearance could reconcile these differences. To test this hypothesis, we examined the longitudinal evolution of cardiac and liver iron in 38 thalassemia major patients, using previously validated magnetic resonance imaging (MRI) techniques. On cross-sectional evaluation, cardiac iron was uncorrelated with liver iron, similar to previous studies. However, relative changes in heart and liver iron were compared with one another using a metric representing the temporal delay between them. Cardiac iron significantly lagged liver iron changes in almost half of the patients, implying a functional but delayed association. The degree of time lag correlated with initial HIC ($r = 0.47$, $P < .003$) and initial cardiac R2* ($r = 0.57$, $P < .001$), but not with patient age. Thus, longitudinal analysis confirms a lag in the loading and unloading of cardiac iron with respect to liver iron, and partially explains the weak cross-sectional association between these parameters. These data reconcile several prior studies and provide both mechanical and clinical insight into cardiac iron accumulation. (Blood. 2008; 112:2973-2978)

Introduction

Despite availability of iron chelation, iron-mediated cardiac toxicity remains the leading cause of death in thalassemia major patients.[1] Cardiac dysfunction, whether detected by radionuclide angiography, echocardiography, or magnetic resonance imaging (MRI), is often a late finding and carries an ominous prognosis.[2,3] Although intense chelation can rescue many patients, depleting cardiac iron burden often takes years and mortality is high with incomplete compliance.[3] Thus, prevention of cardiac iron accumulation and dysfunction is imperative. Initial studies in this area examined hepatic iron concentration (HIC), as measured by liver biopsy, and serum ferritin levels as potential predictors of cardiac toxicity.[4-6] This hypothesis was logical because HIC is an excellent indicator of iron balance and total body iron stores.[6,7] These early studies concluded that elevated liver iron and serum ferritin trends raise prospective risk of cardiac dysfunction, implying a correlation between cardiac and liver iron deposition.[4-6] Based upon this work, treatment algorithms for iron removal therapy based primarily on HIC and ferritin levels[8,9] were developed with the goal of minimizing cardiac and endocrine toxicities.

However, the use of HIC and ferritin to infer cardiac iron has been challenged by recent MRI studies.[10-13] MRI allows organ iron concentrations to be easily and noninvasively measured and has been validated on both animals and humans.[14-16] Cross-sectional analysis has demonstrated poor correlation between HIC or ferritin and cardiac iron.[10-12,13] In addition, some patients develop cardiac deposition and symptoms with relatively minor somatic iron overload.[17-19] These findings have produced a backlash against the use of conventional markers of iron stores to predict cardiac risk.[20,21]

Reconciliation of the disparity between longitudinal and cross-sectional studies requires knowledge of the temporal association of cardiac and liver iron stores. MRI data suggest that the kinetics of iron loading and unloading differ markedly in the 2 organs.[11,22] These kinetic differences may introduce lag between changes in liver and cardiac iron, destroying the cross-sectional correlations between these observations, while preserving a causal relationship. To test the hypothesis that cardiac iron lags changes in liver iron, we evaluated longitudinal heart and liver iron time courses in 38 thalassemia major patients using an objective metric of time delay. We also compared whether patient liver iron was higher at the onset of detectable cardiac iron accumulation ($T2^* < 20$ ms) than at the moment of cardiac iron clearance ($T2^* > 20$ ms).

Methods

We performed a retrospective review of medical records from more than 100 patients with thalassemia major who had MRI examinations for cardiac and liver iron performed at Childrens Hospital Los Angeles (CHLA). Approximately 60% of the patients received thalassemia care at outside institutions, but had their noninvasive iron assessments at CHLA. Permission for medical review and waiver of informed consent according to the Declaration of Helsinki were approved by the IRB Committee on Clinical Investigation at CHLA. There were 38 eligible subjects who underwent 3 or more MRIs within 2002 to 2007 to estimate their heart and liver iron concentration. The mean age of the patients was 20.6 plus or minus 8.9 years (range: 5.4-43.8 years). The average cardiac R2* at first MRI was 80.1 plus or minus 94.5 Hz (median was 37.1 Hz) and the average HIC was 14.7 plus or minus 11.9 mg/g dry weight liver. The average time between a patient's first and last MRI was 3.1 plus or minus 1.2 years (range: 0.9-4.9 years). All patients were on chronic transfusions every 2 to 4 weeks to maintain a pretransfusion hemoglobin level greater than 95 g/L. All of these patients had used deferoxamine for most of their chelation history. At the time of the last MRI reviewed for this study, 8 patients remained on deferoxamine therapy, 28 patients were using deferasirox for an average of

Submitted April 8, 2008; accepted July 3, 2008. Prepublished online as *Blood* First Edition paper, July 23, 2008; DOI 10.1182/blood-2008-04-148767.

The online version of this article contains a data supplement.

The publication costs of this article were defrayed in part by page charge payment. Therefore, and solely to indicate this fact, this article is hereby marked "advertisement" in accordance with 18 USC section 1734.

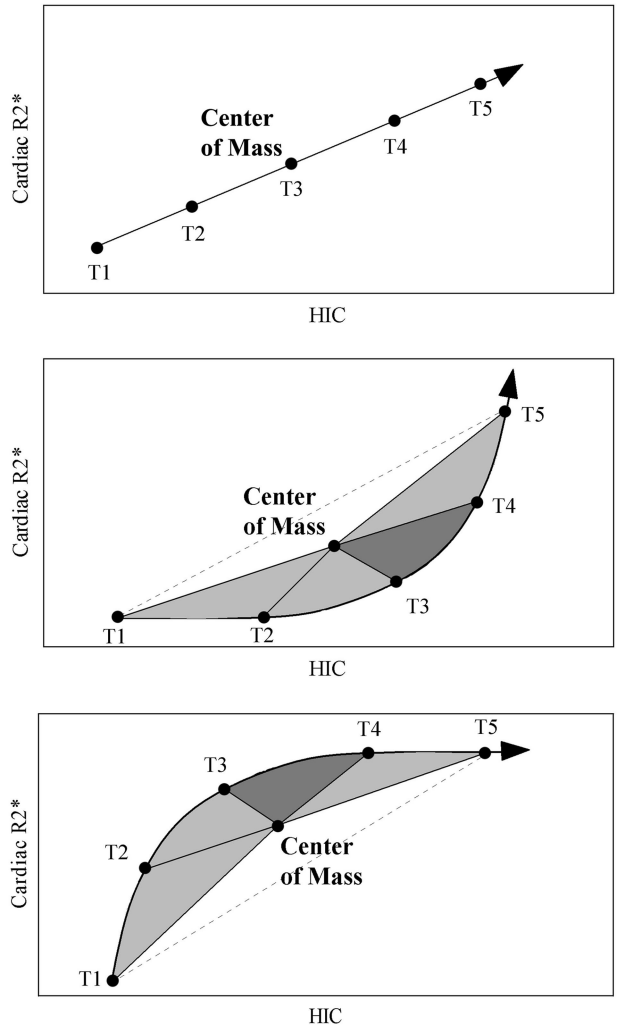

Figure 1. Schematic illustrating time lag detection and quantification. Center of mass is calculated for each time course by finding the average liver iron and cardiac R2* for all of the consecutive time points (T1-T5), and the magnitude (area under the curve) and direction of the time course "rotation" is determined. (Top) No rotation, area = 0: HIC and cardiac R2* have a linear relationship with no delays. (Middle) Counterclockwise (positive) rotation indicates that cardiac R2* lags liver iron changes. (Bottom) Clockwise (negative) rotation indicates that HIC lags cardiac R2*.

1.4 years, 1 patient was using deferiprone for 2.2 years, and 1 patient was on combination therapy of deferiprone and deferoxamine for 5.1 years (Document S1, available on the *Blood* website; see the Supplemental Materials link at the top of the online article). HIC was estimated at intervals ranging from 3 to 18 months using liver R2 and R2* measurements as previously described.[23] Cardiac R2* (equal to 1000/T2*) was also determined by previously validated methods.[24] Although an absolute calibration curve does not exist, in vivo, cardiac R2* has been shown to be directly proportional to iron in animal and autopsy studies.[14,16]

Figure 1 demonstrates the metric used to detect lag between cardiac and liver iron levels. In the top example, heart and liver iron levels at consecutive observations (labeled T1-T5) form a straight line, indicating no temporal delay between these changes. To establish a reproducible reference point, we calculated the center of mass for each time course; the center of mass represents the average liver iron and cardiac R2* for all of the points (T1-T5). Note that the time course passes through the center of mass if there is no time lag between the heart and liver iron.

In the second example, cardiac iron levels lag behind changes in liver iron. To quantify this lag, we can draw segments from each time point to the center of mass. This forms a series of triangles that rotate counterclockwise about the center of mass. The greater the time lag between heart and liver iron, the greater the total triangular area or area under the curve (AUC).

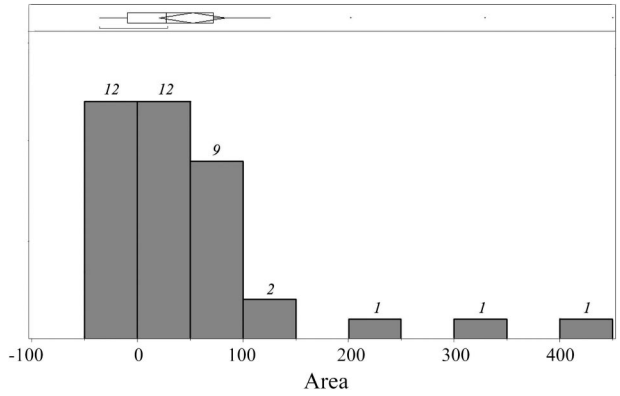

Figure 2. Distribution of area under the curve measured for each of the 38 trajectories. Area under the curve (AUC) represents the magnitude of time lag; the italicized numbers above each bar represent the number of patients having a given AUC. The distribution is badly skewed toward positive trajectories, revealing that cardiac iron significantly lags liver iron in many patients.

Applying this approach to the top example, we can observe that the subtended triangles have zero total area, corresponding to the lack of delay between the parameters. The bottom example illustrates the metric from a time course where liver iron lags cardiac iron. Now, the time points rotate clockwise about the center of mass, instead of counterclockwise; the subtended area again reflects the relative magnitude of the delay. Arbitrarily, we designated counterclockwise rotation (heart lagging liver) to have a positive sign, and clockwise rotation (liver lagging heart) was given a negative sign.

The relative frequency of time courses having positive and negative rotation was compared using Fisher exact test. The relative magnitude of positive and negative AUCs was compared using Wilcoxin signed rank test. AUCs were compared with patient age, initial HIC, and initial cardiac R2* using simple linear regression. HIC values preceding the transitions from undetectable to detectable cardiac iron ($T2^* > 20$ ms to $T2^* < 20$ ms) were compared with HIC values preceding clearance of detectable cardiac iron ($T2^* < 20$ ms to $T2^* > 20$ ms) by Wilcoxin signed rank test. A P value of .05 was deemed significant for all analyses.

Results

Figure 2 is a histogram showing the AUC distribution calculated for 38 time courses; 26 (68.4%) had an overall positive area and 12 (31.6%) had an overall negative area ($P = .16$). However, the distribution was positively skewed (mean = 51.0; median = 25.9) and large areas were observed only in the counterclockwise direction. The magnitude of the positive areas averaged 84.0 (range: 7.4-449), and the magnitude of the negative areas averaged −20.6 (range: −37.2-−6.8); P value less than .006. In fact, 18 (47.3%) of 38 patients had a positive area greater than the largest observed negative area, representing time lags detectable above measurement uncertainties. The magnitude of all of the positive areas represented 89.8% of the total and the magnitude of all of the negative areas represented 10.2% of the total.

To investigate potential predictors of this time lag, AUCs were compared with initial HIC, initial cardiac R2*, and patient age. Greater time lags were observed with greater initial HIC ($r = 0.47$, $P < .003$) and initial cardiac R2* ($r = 0.57$, $P < .001$); no correlation was seen with patient age.

Not only did the time courses rotate counterclockwise individually, they formed loops in the aggregate as well. Figure 3 shows the longitudinal relationship between HIC and cardiac R2* for the entire population. In each time course, the circle represents the initial HIC and R2* measurement and each following point

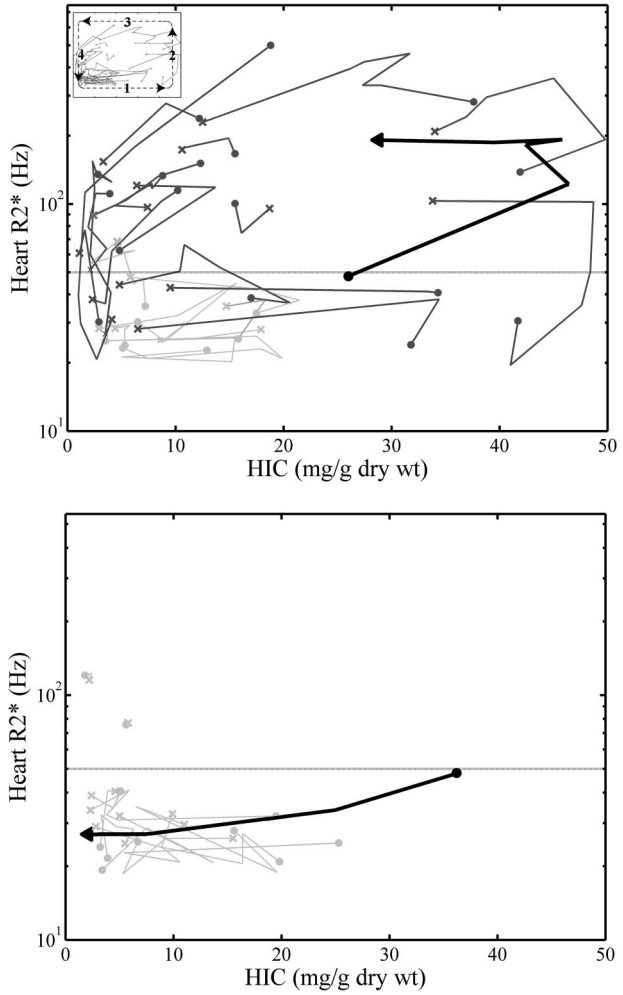

Figure 3. Aggregate of positive (top) and negative (bottom) time courses formed by plotting chronologic HIC and cardiac R2* measurements for 38 subjects. Cardiac R2* (equal to 1000/T2*) is on the vertical axis in log scale; HIC (calculated using liver R2 and R2*) is on the horizontal axis. First and last MRI measurements are denoted by a filled circle and an "x," respectively. In the plot of positive time courses, the time courses having AUCs more than 37.2 (the largest negative AUC) are indicated by dark lines and the smaller AUCs, by light gray lines. The time course indicated by a thick, black line is representative of the counterclockwise movement of these time courses as a whole. The inset in the top left corner shows the numbered "limbs." In the plot of negative time courses, all time courses are shown in light gray except one. The time course indicated by a thick, black line is a representative of the clockwise movement of these time courses as a whole.

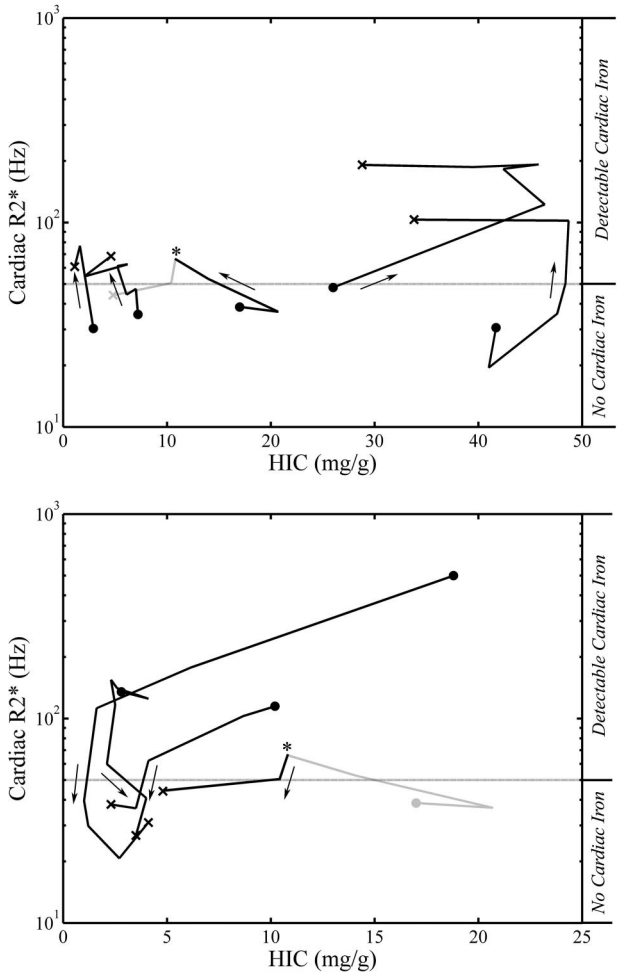

Figure 4. Time courses of patients who transitioned above or below a cardiac R2* of 50 Hz. The time courses of the patients with increasing and decreasing cardiac R2* are shown in the top and bottom panels, respectively. Cardiac R2* (equal to 1000/T2*) is on the vertical axis in log scale; HIC (calculated using liver R2 and R2*) is on the horizontal axis. First and last MRI measurements are denoted by a filled circle and an "x," respectively. These graphs represent 8 patients with 9 transitions. The patient who transitioned above and below an R2* of 50 Hz during the given time is shown in both panels (*). In each panel, only the relevant part of this time course is colored black; the unrelated portion is gray. The arrows indicate the direction of cardiac iron (increasing R2* or decreasing R2*).

represents a chronologic measurement. The x represents the last measurement for that time course. Positive time courses are shown in the top panel and negative time courses in the bottom panel. The 18 positive time courses having AUCs more than 37.2 (the largest negative AUC) are indicated by dark lines and the smaller AUCs in gray. Macroscopically, it is quite apparent that larger positive time courses trace a counterclockwise loop or rectangle, consisting of 4 "limbs," numbered 1 through 4. Limb 1 demonstrates increasing or decreasing HIC with little change in R2*; limb 2 showed increasing R2* with little change in HIC; limb 3 exhibits decreasing HIC with little change in R2*; and limb 4 reveals decreasing R2* with little change in HIC. Notably, there are no time courses going through the middle of the loop, highlighting the nonlinearity of the liver-heart iron relationship. The 53% of trajectories showing weak time lags (AUC < 37.2) either did not have cardiac iron overload or exhibited extremely small changes in cardiac iron, leaving AUC calculation vulnerable to the inherent MRI measurement errors.

If cardiac iron does lag liver iron in both somatic iron loading and unloading, one would expect that the liver iron at which cardiac iron accumulates will be significantly higher than the liver iron level at which the heart clears. To test this hypothesis, we looked at HIC values of patients who transitioned above or below a cardiac R2* of 50 Hz (a T2* of 20 ms, the lower limit of normal). Of the 38 patients analyzed, there were 9 transitions about the critical value (Figure 4). The 5 patients with onset of detectable cardiac iron loading (top panel) had an HIC between 2.3 and 48.4 (median: 15.2) at the time of the transition, whereas the 4 patients who showed clearance of detectable cardiac iron (bottom panel) had an HIC between 1.1 and 9.9 (median: 3.5) at the time of the transition; $P = .14$. One patient transitioned above and below an R2* of 50 Hz during the given time. Although this difference was not statistically significant, perhaps because of small sample size, it suggests that cardiac iron clearance may not occur until liver iron is quite low. In contrast, primary cardiac iron accumulation occurs over an extremely broad range of liver iron concentrations.

Discussion

Although HIC measurements are an excellent gauge of body iron stores and iron balance, the ability of HIC to predict target organ iron toxicity is limited. On cross-sectional evaluation, there is a marked disconnect between liver and heart iron values. This can be easily appreciated in Figure 3, and has been described in several prior studies.[10-13] One reason for this disconnect is organ-specific mechanisms of iron uptake/release. Liver, bone marrow, and spleen are the natural reservoirs for iron, and transferrin-bound iron is shuttled among these stores in a tightly regulated manner. The heart and endocrine glands also have well-regulated transferrin-mediated uptake, but pathologic iron deposition in these organs occurs through unregulated influx of NTBI.[25-27] NTBI levels rise once transferrin is fully saturated and are modulated by the type and duration of chelator exposure.[28]

The different iron uptake mechanisms of heart and liver result in uneven rate of organ iron loading. Transfusional iron burden initially fills the liver through transferrin-mediated uptake; positive and negative iron balance at this stage leads to leftward and rightward movement in limb 1 of Figure 3. Interestingly, some of the patient time courses in this limb still form shallow counterclockwise loops, suggesting fluctuations of cardiac iron within the "normal" range. The physiologic factors responsible for delaying cardiac iron uptake relative to liver iron uptake are unknown. It may be that NTBI levels are initially well controlled through chelation despite high somatic iron burdens. Alternatively, there may be as yet uncharacterized maturational, endocrine, genetic, or metabolic comodulators of cardiac iron uptake.[29-31]

Despite an apparent "delay" in cardiac iron uptake, some patients rapidly increase their cardiac iron at high liver iron concentration (Figure 3 limb 2). Several patients continued to accumulate cardiac iron despite negative liver iron balance, suggesting some degree of momentum or memory to the cardiac iron uptake process. Previous studies have demonstrated a HIC threshold at which chelatable iron and cardiac iron accumulation increase drastically.[32] One possible explanation is that elevated liver iron may damage the liver, inhibiting hepatic NTBI uptake and increasing cardiac NTBI exposure.[33] Alternatively, cell culture work suggests that cardiac iron accumulation up-regulates cardiac iron transport, creating a mechanism for precipitous cardiac iron uptake and uptake memory.[25]

Although these observations suggest that high HIC prospectively predicts cardiac iron loading, low HIC does not necessarily imply low risk for cardiac iron. According to Figure 4, 2 of 5 patients who developed de novo cardiac iron deposition did so with liver iron concentrations less than 6 mg/g. Others have also described primary cardiac iron accumulation in otherwise "low-risk" patients.[17-19] Because most adult thalassemia major patients have fully saturated transferrin, regardless of their liver iron, they remain at risk for cardiac iron accumulation whenever they do not have circulating free chelator.

In addition to differences in iron uptake, there are differences in iron elimination that weaken the cross-sectional relationship between heart and liver iron. Cardiac iron is relatively more difficult to remove than liver iron; the cardiac iron removal rate with deferoxamine is 5 times slower than the liver during intensive chelation.[22] Patients on intensive chelation therapy can move from a state of heavy heart and liver iron burdens to a state of heavy cardiac iron and minimal liver iron burden. Patients in limbs 3 and 4 of Figure 3 demonstrate this type of behavior. Cardiac iron may not significantly decrease until liver iron is quite low; in fact, patients who managed to clear the heart had a median liver iron of 3.5 (Figure 4).

Slow cardiac iron clearance is a major contributor to the curved time course observed macroscopically (Figure 3) and for individual patients (Figure 2). Not surprisingly, time lag was more profound in patients with initially elevated cardiac and liver iron. Many of these high-risk patients receive intense chelation, unmasking the kinetic differences between the heart and the liver because there is less time for equilibration. There is also evidence that cardiac iron is chemically less accessible at higher cardiac iron concentrations.[34]

Although cardiac iron levels seem to lag with respect to HIC during both somatic iron loading and unloading, cardiac iron levels cannot be viewed as passively following liver iron levels. The type and pattern of chelation can affect the heart and liver differently and are vital in influencing the relationship between cardiac and liver iron. For example, it has been demonstrated that the number of deferoxamine doses per year is the strongest predictor of survival, regardless of ferritin levels.[35] The success of continuous deferoxamine lies in its ability to continuously suppress NTBI, not in the delivery of greater amount of drug.[36,37] The pattern of drug administration is important for oral chelation as well. In the gerbil, dividing deferasirox into 2 doses per day instead of the same dose once per day significantly increased cardiac iron removal relative to the liver.[38] The data presented in this paper predominantly reflect subcutaneous, intermittent deferoxamine chelation therapy (61% of chelation-years), compared with deferasirox (33% of chelation-years) and deferiprone (6% of chelation-years). Deferiprone, in particular, may lower cardiac iron with less change in hepatic iron concentration, but our study was too small and unbalanced among the chelators to make any comparison in this regard.[39,40]

This present work suffered from several other limitations as well. The study was observational and patients had wide ranges of ages, iron loading, and chelation compliance. MRI study intervals varied among individual patients. The relatively small sample size limited the number of patients in a given cardiac iron and liver iron range, as well as the number of patients who crossed the R2* of 50-Hz threshold. Because some of the patients had comprehensive care elsewhere, we had incomplete data regarding transfusional burden, past medical care, and chelation compliance. Referral patterns may have also biased the study population toward greater iron burdens. Despite the variability introduced by these shortcomings, clear and statistically significant patterns were identified in cardiac and liver iron parameters. Another limitation is the choice of the T2* threshold to designate presence or absence of cardiac iron. Cardiac iron is never actually cleared from the heart; it is necessary for normal heart function, but varies continuously with cardiac 1/T2* in all subjects. Because pathologic amounts of iron must be distinguished from physiologic fluctuations in iron levels and weak noniron modulators of cardiac T2*, a cutoff of 20 ms is the generally accepted threshold for "detectable" cardiac iron. Like any threshold, it is imperfect, and a certain percentage of patients in the range 20 to 25 ms will have mild cardiac iron overload; we typically report these patients as having borderline T2* values.[1,33] We used the 20-ms threshold to demarcate the onset of MRI-recognizable cardiac iron accumulation and clearance, but the concepts would have been similar for a different threshold choice. Lastly, the AUC metric that we used to detect the lag between cardiac and liver iron loading is ad hoc and cannot be used to derive pharmacokinetic information regarding organ iron loading or removal. Because liver iron can respond with a half-life of 2 to 3 months, our clinical practice of annual MRI examinations may

undersample the true time course of heart and liver iron, underestimating the time lag severity.

Despite these limitations, the present data have clinical implications in addition to offering mechanistic insight. For example, although high liver iron levels appear to increase the risk of severe cardiac iron accumulation, there is simply no safe lower liver iron concentration that guarantees cardiac protection. As a result, regular cardiac MRI screening is a vital component in chelation monitoring. The present data also reinforce that cardiac iron clearance is slow, emphasizing the need for primary prevention of cardiac iron overload. Adequate protection depends on the type and pattern of iron chelation just as much as the total chelator dose and liver iron levels. Most importantly, regular clinical monitoring of hepatic and cardiac iron is essential for primary prevention. Better understanding of these contributing factors will lead to improved clinical guidelines for cardioprotection.

Acknowledgments

We are grateful to Debbie Harris, Trish Peterson, Paola Pederzoli, Colleen McCarthy, Janelle Miller, Thomas Hofstra, and Susan Claster for their support of the MRI program. We would also like to thank Nancy Sweeters, Ellen Butensky, Paul Harmatz, and Elliot Vichinsky from Childrens Hospital Oakland for their help with subject recruitment. We would also like to acknowledge Dr Michael Tyszka at the California Institute of Technology for his helpful discussions on the mathematical formalism used in this paper.

This work was supported by the National Heart, Lung, and Blood Institute (Bethesda, MD; 1 RO1 HL075592-01A1), General Clinical Research Center at the Children's Hospital Los Angeles (RR000043-43), Centers for Disease Control (Thalassemia Center Grant U27/CCU922106; Atlanta, GA), Novartis Pharma (East Hanover, NJ), and the Department of Pediatrics, Childrens Hospital Los Angeles (Los Angeles, CA).

Authorship

Contribution: L.J.N. performed research, analyzed data, and wrote the paper. S.M.C., A.S.N., and T.D.C. collected data and assisted in writing; and J.C.W. designed and performed research, analyzed data, and wrote the paper.

Conflict-of-interest disclosure: S.M.C. is a member of the Novartis speaker's bureau for deferasirox. T.D.C. has received research funding and honoraria from Novartis and has received honoraria from Apotex (Weston, ON). J.C.W. is a consultant to and has received research funding and honoraria from Novartis, and has received honoraria from Apotex (Weston, ON). All other authors declare no competing financial interests.

Correspondence: John C. Wood, Childrens Hospital Los Angeles, Division of Cardiology, 4650 Sunset Boulevard, Los Angeles, CA 90027; e-mail: jwood@chla.usc.edu.

References

1. Borgna-Pignatti C, Rugolotto S, De Stefano P, et al. Survival and complications in patients with thalassemia major treated with transfusion and deferoxamine. Haematologica. 2004;89:1187-1193.
2. Wood JC, Enriquez C, Ghugre N, et al. Physiology and pathophysiology of iron cardiomyopathy in thalassemia. Ann N Y Acad Sci. 2005;1054:386-395.
3. Davis BA, O'Sullivan C, Jarritt PH, Porter JB. Value of sequential monitoring of left ventricular ejection fraction in the management of thalassemia major. Blood. 2004;104:263-269.
4. Olivieri NF, Nathan DG, MacMillan JH, et al. Survival in medically treated patients with homozygous beta-thalassemia. N Engl J Med. 1994;331:574-578.
5. Telfer PT, Prestcott E, Holden S, Walker M, Hoffbrand AV, Wonke B. Hepatic iron concentration combined with long-term monitoring of serum ferritin to predict complications of iron overload in thalassaemia major. Br J Haematol. 2000;110:971-977.
6. Brittenham GM, Griffith PM, Nienhuis AW, et al. Efficacy of deferoxamine in preventing complications of iron overload in patients with thalassemia major. N Engl J Med. 1994;331:567-573.
7. Angelucci E, Brittenham GM, McLaren CE, et al. Hepatic iron concentration and total body iron stores in thalassemia major. N Engl J Med. 2000;343:327-331.
8. Olivieri NF, Brittenham GM. Iron-chelating therapy and the treatment of thalassemia. Blood. 1997;89:739-761.
9. Porter JB, Davis BA. Monitoring chelation therapy to achieve optimal outcome in the treatment of thalassaemia. Best Pract Res Clin Haematol. 2002;15:329-368.
10. Tanner MA, Galanello R, Dessi C, et al. Myocardial iron loading in patients with thalassemia major on deferoxamine chelation. J Cardiovasc Magn Reson. 2006;8:543-547.
11. Wood JC, Tyszka JM, Ghugre N, Carson S, Nelson MD, Coates TD. Myocardial iron loading in transfusion-dependent thalassemia and sickle-cell disease. Blood. 2004;103:1934-1936.
12. Aessopos A, Fragodimitri C, Karabatsos F, et al. Cardiac magnetic resonance imaging R2* assessments and analysis of historical parameters in patients with transfusion-dependent thalassemia. Haematologica. 2007;92:131-132.
13. Anderson LJ, Holden S, Davis B, et al. Cardiovascular T2-star (T2*) magnetic resonance for the early diagnosis of myocardial iron overload. Eur Heart J. 2001;22:2171-2179.
14. Wood JC, Otto-Duessel M, Aguilar M, et al. Cardiac iron determines cardiac T2*, T2, and T1 in the gerbil model of iron cardiomyopathy. Circulation. 2005;112:535-543.
15. Wang ZJ, Lian L, Chen Q, Zhao H, Asakura T, Cohen AR. 1/T2 and magnetic susceptibility measurements in a gerbil cardiac iron overload model. Radiology. 2005;234:749-755.
16. Ghugre NR, Enriquez CM, Gonzalez I, Nelson MD Jr, Coates TD, Wood JC. MRI detects myocardial iron in the human heart. Magn Reson Med. 2006;56:681-686.
17. Anderson LJ, Westwood MA, Prescott E, Walker JM, Pennell DJ, Wonke B. Development of thalassaemic iron overload cardiomyopathy despite low liver iron levels and meticulous compliance to desferrioxamine. Acta Haematol. 2006;115:106-108.
18. Kolnagou A, Economides C, Eracleous E, Kontoghiorghes GJ. Low serum ferritin levels are misleading for detecting cardiac iron overload and increase the risk of cardiomyopathy in thalassemia patients: the importance of cardiac iron overload monitoring using magnetic resonance imaging T2 and T2*. Hemoglobin. 2006;30:219-227.
19. Wood JC. Magnetic resonance imaging measurement of iron overload. Curr Opin Hematol. 2007;14:183-190.
20. Aessopos A, Berdoukas V, Tsironi M. The heart in transfusion dependent homozygous thalassaemia today: prediction, prevention and management. Eur J Haematol. 2008;80:93-106.
21. Berdoukas V, Dakin C, Freema A, Fraser I, Aessopos A, Bohane T. Lack of correlation between iron overload cardiac dysfunction and needle liver biopsy iron concentration. Haematologica. 2005;90:685-686.
22. Anderson LJ, Westwood MA, Holden S, et al. Myocardial iron clearance during reversal of siderotic cardiomyopathy with intravenous desferrioxamine: a prospective study using T2* cardiovascular magnetic resonance. Br J Haematol. 2004;127:348-355.
23. Wood JC, Enriquez C, Ghugre N, et al. MRI R2 and R2* mapping accurately estimates hepatic iron concentration in transfusion-dependent thalassemia and sickle cell disease patients. Blood. 2005;106:1460-1465.
24. Ghugre NR, Enriquez CM, Coates TD, Nelson MD Jr, Wood JC. Improved R2* measurements in myocardial iron overload. J Magn Reson Imaging. 2006;23:9-16.
25. Parkes JG, Hussain RA, Olivieri NF, Templeton DM. Effects of iron loading on uptake, speciation, and chelation of iron in cultured myocardial cells. J Lab Clin Med. 1993;122:36-47.
26. Oudit GY, Sun H, Trivieri MG, et al. L-type Ca(2+) channels provide a major pathway for iron entry into cardiomyocytes in iron-overload cardiomyopathy. Nat Med. 2003;9:1187-1194.
27. Randell EW, Parkes JG, Olivieri NF, Templeton DM. Uptake of non-transferrin-bound iron by both reductive and nonreductive processes is modulated by intracellular iron. J Biol Chem. 1994;269:16046-16053.
28. Cabantchik ZI, Breuer W, Zanninelli G, Cianciulli P. LPI-labile plasma iron in iron overload. Best Pract Res Clin Haematol. 2005;18:277-287.
29. Wu KH, Chang JG, Ho YJ, Wu SF, Peng CT. Glutathione S-transferase M1 gene polymorphisms are associated with cardiac iron deposition in patients with beta-thalassemia major. Hemoglobin. 2006;30:251-256.

30. Wood JC, Claster S, Carson S, et al. Vitamin D deficiency, cardiac iron, and cardiac function in thalassemia major. Br J Haematol. 2008;141:891-894.
31. Wood JC, Origa R, Agus A, Matta G, Coates TD, Galanello R. Onset of cardiac iron loading in pediatric patients with thalassemia major. Haematologica. 2008;93:917-920.
32. Jensen PD, Jensen FT, Christensen T, Eiskjaer H, Baandrup U, Nielsen JL. Evaluation of myocardial iron by magnetic resonance imaging during iron chelation therapy with deferrioxamine: indication of close relation between myocardial iron content and chelatable iron pool. Blood. 2003;101:4632-4639.
33. Scheiber-Mojdehkar B, Zimmermann I, Dresow B, Goldenberg H. Differential response of non-transferrin bound iron uptake in rat liver cells on long-term and short-term treatment with iron. J Hepatol. 1999;31:61-70.
34. Shiloh H, Iancu TC, Bauminger ER, Link G, Pinson A, Hershko C. Deferoxamine-induced iron mobilization and redistribution of myocardial iron in cultured rat heart cells: studies of the chelatable iron pool by electron microscopy and Mossbauer spectroscopy. J Lab Clin Med. 1992;119:428-436.
35. Gabutti V, Piga A. Results of long-term iron-chelating therapy. Acta Haematol. 1996;95:26-36.
36. Davis BA, Porter JB. Long-term outcome of continuous 24-hour deferoxamine infusion via indwelling intravenous catheters in high-risk beta-thalassemia. Blood. 2000;95:1229-1236.
37. Porter JB, Abeysinghe RD, Marshall L, Hider RC, Singh S. Kinetics of removal and reappearance of non-transferrin-bound plasma iron with deferoxamine therapy. Blood. 1996;88:705-713.
38. Otto-Duessel M, Aguilar M, Nick H, Moats R, Wood JC. Comparison of twice-daily vs once-daily deferasirox dosing in a gerbil model of iron cardiomyopathy. Exp Hematol. 2007;35:1069-1073.
39. Anderson LJ, Wonke B, Prescott E, Holden S, Walker JM, Pennell DJ. Comparison of effects of oral deferiprone and subcutaneous desferrioxamine on myocardial iron concentrations and ventricular function in beta-thalassemia. Lancet. 2002;360:516-520.
40. Pennell DJ, Berdoukas V, Karagiorga M, et al. Randomized controlled trial of deferiprone or deferoxamine in beta-thalassemia major patients with asymptomatic myocardial siderosis. Blood. 2006;107:3738-3744.